Global Journal of Engineering and Technology Advances

eISSN: 2582-5003

Cross Ref DOI: 10.30574/gjeta

Journal homepage: https://gjeta.com/

GJETA

(Review Article)

Check for updates

MHD flow properties due to a porous rotating disk in a mixed convective fluid flow with buoyancy and radiation

Raphael Ehikhuemhen Asibor [1,*] and Celestine Friday Osudia [2]

[1] *Department of Computer Science/Mathematics, Igbinedion University Okada, Edo State, Nigeria.*
[2] *Department of Mathematics, Delta State Post Primary Education Board, Asaba, Nigeria.*

Global Journal of Engineering and Technology Advances, 2023, 14(03), 061–075

Publication history: Received on 02 February 2023; revised on 12 March 2023; accepted on 15 March 2023

Article DOI: https://doi.org/10.30574/gjeta.2023.14.3.0052

Abstract

The importance and differs applications of Magnetohydrodynamics, MHD and mixed convective flow through a porous medium has led to investigation of buoyancy force and thermal radiation on the flow. The modeled ordinary differential equations were transformed by means of similarity transformation into partial differential equations. The resulting equations were solved using Nachtsheim–Swigert iteration technique. The obtained results were conformed to existing ones, and displayed on tables and through graphs. In conclusion the investigated parameters have significant effects on the flow. Close to the boundary positive values of γ is found to give rise to the familiar inflection point profile leading to the destabilization of the laminar flow. Strong injection also leads to the similar destabilization effect. Also, hall parameter m has an interesting effect on the radial and axial velocity profiles. For large values of $m(> 2.0)$, the resistive effects of the magnetic field are diminished and hence the radial and axial velocity profiles decrease with the increase of m, among others.

Keywords: MHD Flow; Porous Medium; Rotating Disk; Mixed Convective Flow; Buoyancy; Radiation

1. Introduction

Rotating disk flow along with heat transfer is one of the classical problems of fluid mechanics, which has both theoretical and practical value. The importance of heat transfer from a rotating body can be ascertained in cases of various types of machinery, for example computer disk derives (see [1]) and gas turbine rotors (see [2]). The rotating-disk problem was first formulated by von-Karmann [3]. He has shown that Navier–Stokes equations of steady flow of a viscous incompressible fluid due to an infinite rotating disk can be reduced to a set of ordinary differential equations and solved them by approximate integral method. But Cochran [4] pointed out that von-Karmans momentum integral solution contained errors. He obtained more accurate results by patching two series expansions. It has been found that the disk acts like a centrifugal fan and hence the fluid near the surface being thrown radially upwards. This in turn generates an axial flow towards the disk to maintain continuity. Benton [5], further improved Cochrans solution and extended the hydrodynamic problem to the flow starting impulsively from rest. The rotationally symmetric flow in presence of an infinite rotating disk with different angular velocity was studied by Roger and Lance [6].

Following a suggestion made by Batchelor [7], Stuart [8] investigated the effect of uniform suction of fluid from the surface of a rotating disk. Suction essentially decreases both the radial and azimuthal components of velocity but increases the axial flow towards the disk at infinity. As a consequence, the boundary layer becomes thinner. Ockendon [9] used asymptotic method to determine the solutions of the problem for small values of suction parameter in case of a rotating disk in a rotating fluid. On the other hand, the effect of uniform blowing through a rotating porous disk on the flow induced by this disk was studied by Kuiken [10].

* Corresponding author: Raphael Ehikhuemhen Asibor

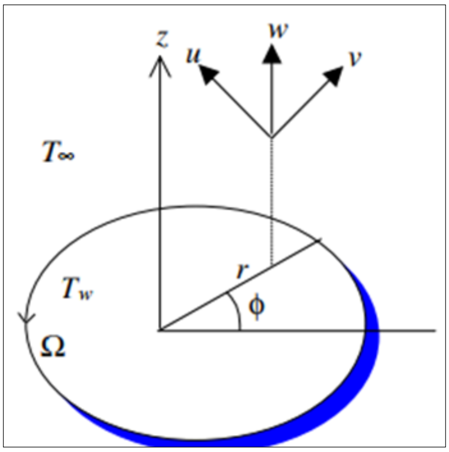

Figure 1 The flow conFigureuration and the coordinate system.

Some interesting results on the effects of the magnetic field on the steady flow due to the rotation of a disk of infinite or finite extent was pointed out by El-Mistikawy et al. [11,12]. Hassan and Attia [13] investigated the steady magneto-hydrodynamic boundary layer flow due to an infinite disk rotating with uniform angular velocity in the presence of an axial magnetic field. They neglected the induced magnetic field but considered Hall current and accordingly solved steady state equations numerically using finite difference approximation. Attia [14] investigated the effects of suction as well as injection along with effects of magnetic field in a flow near a rotating porous disk. It was observed by him that strong injection tends to destabilize the laminar boundary layer but when magnetic field works along with even strong injection, it stabilizes the boundary layer.

In all the above studies to the authors knowledge, constant properties of fluid were not assumed. However, it is known that these physical properties may change significantly with temperature of the flow. To predict the flow behavior accurately, it may be necessary to take into account these variable properties. In this light Zakerullah and Ackroyd [15] investigated the free convection flow above a horizontal circular disk for variable fluid properties. Herwig [16] analyzed the influence of variable properties on laminar fully developed pipe flow with constant heat flux across the wall. It was shown
how the exponents in the property ratio method depend on the fluid properties. The influence of temperature dependent fluid properties on laminar boundary layers was examined by Herwig and Wickern [17] for wedge flow. In case of fully developed laminar flow in concentric annuli, the effect of the variable property has been studied by Herwig and Klemp [18]. Herwig [19] studied the laminar film boiling including variable properties.

In the present paper, the steady MHD laminar flow of a viscous conducting, compressible flow due to a porous rotating disk of infinite extend is studied in the presence of an external uniform magnetic field directed perpendicular to the disk taking the properties of the fluid as strong functions of temperature. A uniform suction or injection through the disk is considered for the whole range of suction or injection velocities. The governing non-linear partial differential equations are integrated numerically using Nachtsheim and Swigert [20] iteration technique.

2. Basic equations

Consider the steady MHD laminar boundary layer flow due to a rotating disk in an electrically conducting viscous compressible fluid in the presence of an external magnetic field and Hall current. The equations governing the fluid flow are

Equation of continuity:

$$\nabla \cdot (\rho q) = 0 \quad \dots\dots\dots\dots\dots (1)$$

Navier–Stokes equation:

$$\rho(q \cdot \nabla)q = -\nabla p + [\nabla \cdot (\mu\nabla)]q + (J \times B), \dots\dots\dots\dots\dots (2)$$

The generalized Ohm's law:

$$J = \sigma[E + q \times B - \beta(J \times B)], \dots\dots\dots\dots\dots (3)$$

Energy equation :

$$\rho C_p\big((q\cdot\nabla)\big)T = \nabla\cdot(\kappa\nabla)T \quad \dots\dots\dots\dots\dots(4)$$

The external uniform magnetic field is applied perpendicular to the plane of the disk and has a constant magnetic flux density $B = (0,0,B_0)$ which is assumed unaltered by taking magnetic Reynolds number $Re_m \ll 1$. E is the electric field which results from charge separation and is in the z −direction. Eq. (3) expresses the Hall effect, where $\beta = 1/ne$ is the Hall factor, n is the electron concentration per unit volume and e is the charge of electron. In Eq. (4), we neglected the viscous energy dissipation, Joule heating term and the heat generation/absorption coefficient.

3. Governing equations

Using non-rotating cylindrical polar coordinates (r,ϕ,z), the disk rotates with constant angular velocity Ω and is placed at $z = 0$, and the fluid occupies the region $z > 0$, where z is the vertical axis in the cylindrical coordinates system with r and ϕ as the radial and tangential axes respectively. The components of the flow velocity q are (u,v,w) in the directions of increasing (r,ϕ,z) respectively, the pressure is P and the density of the fluid is ρ. T is the fluid temperature and the surface of the rotating disk is maintained at a uniform temperature T_w. Far away from the wall, the free stream is kept at a constant temperature T_∞ and at a constant pressure, P_∞. The fluid is assumed to be Newtonian, viscous and electrically conducting. The external uniform magnetic field is applied perpendicular to the surface of the disk and has a constant magnetic flux density B_0 which is assumed unchanged by taking small magnetic Reynolds number ($Re_m \ll 1$). The electron–atom collision frequency is assumed to be relatively high, so that the Hall Effect is assumed to exist. We assume that the fluid properties, viscosity (μ) and thermal conductivity (κ) coefficients and density (ρ) are functions of temperature alone and obey the following laws [21]:

$$\mu = \mu_\infty\left[\frac{T}{T_\infty}\right]^a, \kappa = \kappa_\infty\left[\frac{T}{T_\infty}\right]^b, D_m = D_\infty\left[\frac{T}{T_\infty}\right]^c, \rho = \rho_\infty\left[\frac{T}{T_\infty}\right]^d \quad \dots\dots\dots\dots\dots(5)$$

Where the a, b and d are arbitrary exponents, κ_∞ is an uniform thermal conductivity of heat and l1 is a uniform viscosity of a fluid. For the present analysis fluid considered is flue gas. For flue gases the values of the exponents a, b and d are taken as $a = 0.7, b = 0.83$ and $d = -1.0$. The physical model and geometrical coordinates are shown in Figure. 1. Due to steady axially symmetric, compressible MHD laminar flow of a homogeneous fluid the governing equations take the following form from Eq. (1)–(4) as:

$$\frac{\partial}{\partial r}(\rho r u) + \frac{\partial}{\partial z}(\rho r w) = 0 \quad \dots\dots\dots\dots\dots(6)$$

$$\begin{aligned}\rho\left(u\frac{\partial u}{\partial r} - \frac{v^2}{r} + w\frac{\partial u}{\partial z}\right) &= -\frac{\partial p}{\partial r} + \frac{\partial}{\partial r}\left(\mu\frac{\partial u}{\partial r}\right) + \frac{\partial}{\partial r}\left(\mu\frac{u}{r}\right) + \frac{\partial}{\partial z}\left(\mu\frac{\partial u}{\partial z}\right)\\ &+Grt(T-T_\infty) + Grc(C-C_\infty) - \frac{\sigma B_0^2}{(1+m^2)}(u-mv),\end{aligned} \quad \dots\dots\dots\dots\dots(7)$$

$$\begin{aligned}\rho\left(u\frac{\partial v}{\partial r} + \frac{uv}{r} + w\frac{\partial v}{\partial z}\right) &= \frac{\partial}{\partial r}\left(\mu\frac{\partial v}{\partial r}\right) + \frac{\partial}{\partial r}\left(\mu\frac{v}{r}\right) + \frac{\partial}{\partial z}\left(\mu\frac{\partial v}{\partial z}\right) + Grt(T-T_\infty)\\ &+Grc(C-C_\infty) - \frac{\sigma B_0^2}{(1+m^2)}(v+mu),\end{aligned} \quad \dots\dots\dots\dots\dots(8)$$

$$\rho\left(u\frac{\partial w}{\partial r} + w\frac{\partial w}{\partial z}\right) = -\frac{\partial p}{\partial z} + \frac{\partial}{\partial r}\left(\mu\frac{\partial w}{\partial r}\right) + \frac{1}{r}\frac{\partial}{\partial r}(\mu w) + \frac{\partial}{\partial z}\left(\mu\frac{\partial w}{\partial z}\right), \dots\dots\dots\dots\dots(9)$$

$$\rho C_p\left(u\frac{\partial T}{\partial r} + w\frac{\partial T}{\partial z}\right) = \frac{\partial}{\partial r}\left(\kappa\frac{\partial T}{\partial r}\right) + \frac{\kappa}{r}\frac{\partial T}{\partial r} + \frac{\partial}{\partial z}\left(\kappa\frac{\partial T}{\partial z}\right) + A(T-T_\infty) - \frac{\partial q_r}{\partial z}, \dots\dots\dots\dots\dots(10)$$

$$\rho\left(u\frac{\partial C}{\partial r} + w\frac{\partial C}{\partial z}\right) = \frac{\partial}{\partial r}\left(D_m\frac{\partial C}{\partial r}\right) + \frac{D_m}{r}\frac{\partial C}{\partial r} + \frac{\partial}{\partial z}\left(D_m\frac{\partial C}{\partial z}\right) - Q(C-C_\infty), \dots\dots\dots\dots\dots(11)$$

here, σ is the electrical conductivity, Cp is the specific heat at constant pressure and m is the Hall current.

When the free path velocity of the fluid particle is comparable to the characteristic dimensions of the flow field domain, Navier-Stokes equations break down since the assumption of continuum media fails. In the range of 0.1<kn<10 of Knudsen Number, the higher order continuum equation, e.g. Burnett equation should be used. For range of 0.001<=Kn<=0.1, no-slip boundary conditions cannot be used and should be replaced with the following expression (God-el-Hak 1999):

$$U_t = \frac{2-\xi}{\xi}\lambda\frac{\partial U_t}{\partial n}$$

Where U_t is the tangent velocity, n is the normal direction to the wall, ξ is the tangent momentum accommodation coefficient and λ is the mean free path. For Kn<0.001, the no-slip boundary condition is valid, therefore, the velocity at the surface is equal to zero. In the present study, we incorporate both the slip and no-slip regims of the Knudsen number that lies in the range $0.1 > Kn > 0$ is considered. Considering the above analysis, the appropriate boundary conditions for the flow induced by an infinite disk ($z = 0$) which is started impulsively into steady rotation with constant angular velocity Ω and a uniform suction/injection w_w through the disk, are given by

$$\left.\begin{array}{c} u = \frac{2-\xi}{\xi}\lambda\frac{\partial u}{\partial z}, v = \Omega r + \frac{2-\xi}{\xi}\square\frac{\partial u}{\partial z}, w = w_w, T = T_w, C = C_e \text{ at } z = 0 \\ u \to 0, v \to 0, T \to T_\infty, C \to C_\infty, p \to p_\infty \text{ as } z \to \infty \end{array}\right\} \ldots\ldots\ldots\ldots\ldots(12)$$

Using the Roseland approximation for radiative heat transfer and the Roseland approximation for diffusion, the expression for the radiative heat flux q_r can be given as

$$q_r = \left(\frac{-4\sigma}{3k_s}\right)\left(\frac{\partial T^4}{\partial y}\right) \ldots\ldots\ldots\ldots\ldots(13)$$

Here in Eq.(9), the parameters σ and k_s represent the Stefan Boltzmann constant and the Roseland mean absorption coefficient, respectively.

Now on assuming that the temperature differences within the fluid flow are sufficiently small, T^4 in Eq.(9) can be expressed as a linear function of $\square_\infty$ ' using the Taylor series expansion. The Taylor series expansion of T^4about T_∞ , after neglecting the higher order terms, takes the form

$$T^4 \cong 4T_\infty^3 T - 3T_\infty^4 \ldots\ldots\ldots\ldots\ldots(14)$$

Thus by (9) and (10), equation () becomes

$$\rho C_p\left(u\frac{\partial T}{\partial r} + w\frac{\partial T}{\partial z}\right) = \frac{\partial}{\partial r}\left(\kappa\frac{\partial T}{\partial r}\right) + \frac{\kappa}{r}\frac{\partial T}{\partial r} + \frac{\partial}{\partial z}\left(\kappa\frac{\partial T}{\partial z}\right) + \left(\frac{16\sigma T_\infty^3}{3k_s}\right)\frac{\partial^2 T}{\partial y^2}, \ldots\ldots\ldots\ldots\ldots(15)$$

4. Similarity transformations

To obtain the solutions of the governing equations, following von-Karmann, a dimensionless normal distance from the disk, $\eta = z(\Omega/v_\infty)^{1/2}$ is introduced along with the following representations for the radial, tangential and axial velocities, pressure and temperature distributions:

$$\begin{array}{c} u = \Omega r F(\eta), v = \Omega r G(\eta), w = (\Omega \nu_\infty)^{\frac{1}{2}} H(\eta), p - p_\infty = 2\mu_\infty \Omega P(\eta), \\ T - T_w = (T - T_\infty)\theta(\eta), C - C_w = (C - C_\infty)\phi(\eta) \end{array} \ldots\ldots\ldots\ldots\ldots(16)$$

where v_∞ is a uniform kinematic viscosity of the fluid. Eqs. (6)–(8) and (10) in this case reduce to the system

$$H' + 2F + H\theta'(1+\gamma\theta)^{-1}d = 0 \ldots\ldots\ldots\ldots\ldots(17)$$

$$\begin{array}{l} F'' + a\gamma(1+\gamma\theta)^{-1}\theta' F' - [F^2 - G^2 + HF'](1+\gamma\theta)^{d-a} \\ -\frac{M}{1+m^2}(F - mG)(1+\gamma\theta)^{-a} + Grt\theta + Grc\phi \; (14) = 0 \end{array} \ldots\ldots\ldots\ldots\ldots(18)$$

$$G'' + a\gamma(1+\gamma\theta)^{-1}\theta' G' - [2FG + HG'](1+\gamma\theta)^{d-a} - \frac{M}{1+m^2}(G+mF)(1+\gamma\theta)^{-a} + Grt\theta + Grc\phi = 0 \quad \ldots\ldots\ldots\ldots\ldots (19)$$

$$\theta'' + b\gamma(1+\gamma\theta)^{-1}\theta'^2 - PrH\theta'(1+\gamma\theta)^{d-b} + \frac{Pr4}{3R}(1+\gamma\theta)^{-b}\theta'' + Pr\delta\theta(1+\gamma\theta)^{-b} = 0 \quad \ldots\ldots\ldots\ldots\ldots (20)$$

$$\phi'' + c\gamma(1+\gamma\theta)^{-1}\phi'\theta' - ScH\phi'(1+\gamma\theta)^{d-c} + \alpha\phi(1+\gamma\theta)^{-c} = 0 \quad \ldots\ldots\ldots\ldots\ldots (21)$$

The boundary conditions (11) transform to

$$F(0) = \gamma F', G(0) = 1 + \gamma G', H(0) = W_s, \theta'(0) = Bi(\theta(0) - 1), \phi'(0) = Ai(\phi(0) - 1), \quad F(\infty) \to 0, G(\infty) \to 0, \theta(\infty) \to 0, \phi(\infty) \to 0 \quad \ldots\ldots\ldots\ldots\ldots (22)$$

5. Surface Wall Transfer

The skin friction coefficients and the rate of heat transfer to the surface, which are of chief physical interest, are also calculated out. The action of the variable properties in the fluid adjacent to the disk sets up a tangential shear stress, which opposes the rotation of the disk. As a consequence, it is necessary to provide a torque at the shaft to maintain a steady rotation. To find the tangential shear stress τ_t and surface (radial) stress τ_r, we apply the Newtonian formulae:

$$\tau_t = \left[\mu\frac{\partial v}{\partial z} + \frac{1}{r}\frac{\partial w}{\partial \vartheta}\right]_{z=0} = \mu_\infty(1+\gamma)^a RE^{\frac{1}{2}}\Omega G'(0) \quad \ldots\ldots\ldots\ldots\ldots (23)$$

and

$$\tau_r = \left[\mu\frac{\partial u}{\partial z} + \frac{\partial w}{\partial r}\right]_{z=0} = \mu_\infty(1+\gamma)^a RE^{\frac{1}{2}}\Omega F'(0) \quad \ldots\ldots\ldots\ldots\ldots (24)$$

Hence the tangential and radial skin-frictions are respectively given by

$$(1+\gamma)^a RE^{\frac{1}{2}} C_{f_t} = G'(0),$$

$$(1+\gamma)^a RE^{\frac{1}{2}} C_{f_r} = F'(0), \quad \ldots\ldots\ldots\ldots\ldots (25)$$

The rate of heat and mass transfer from the disk surface to the fluid is computed by the application of Fouriers law as given below

$$q = -\left(\kappa\frac{\partial T}{\partial z}\right)_{z=0} = -\kappa_\infty \Delta T(1+\gamma)^b \left(\frac{\Omega}{\nu_\infty}\right)^{\frac{1}{2}}\theta'(0)$$

$$J = -\left(Dm\frac{\partial C}{\partial z}\right)_{z=0} = -D_\infty \Delta C(1+\gamma)^c \left(\frac{\Omega}{\nu_\infty}\right)^{\frac{1}{2}}\phi'(0) \quad \ldots\ldots\ldots\ldots\ldots (26)$$

Hence the Nusselt number (Nu) and Sherwood number (Sh) are obtained as

$$(1+\gamma)^{-b} Re^{-\frac{1}{2}} Nu = -\theta'(0)$$

$$(1+\gamma)^{-c} Re^{-\frac{1}{2}} Sh = -\phi'(0) \quad \ldots\ldots\ldots\ldots\ldots (27)$$

where $Re(= \Omega r^2/\nu_\infty)$ is the rotational Reynolds number. In Eqs. (18)–(20), the gradient values of G, F, θ and ϕ at the surface are evaluated when the corresponding differential equations are solved satisfying the convergence criteria.

$$M = \sigma B_0^2/\Omega\rho_\infty, Pr = \mu_\infty C_p/\kappa_\infty, \gamma = (T_w - T_\infty)/T_\infty, W = w_w/\sqrt{\nu_\infty\Omega}$$

$$W_s < 0 \Longrightarrow \text{suction}, W_s > 0 \ \Longrightarrow \text{injection at the surface}$$

6. Solutions

Numerical solutions to the transformed set of coupled, nonlinear, differential Eqs. (13) – (16) were obtained, utilizing a modification of the program suggested by Nachtsheim and Swigert. Within the context of the initial value method and the Nachtsheim–Swigert iteration technique the outer boundary conditions may be functionally represented by the first order Taylors series as

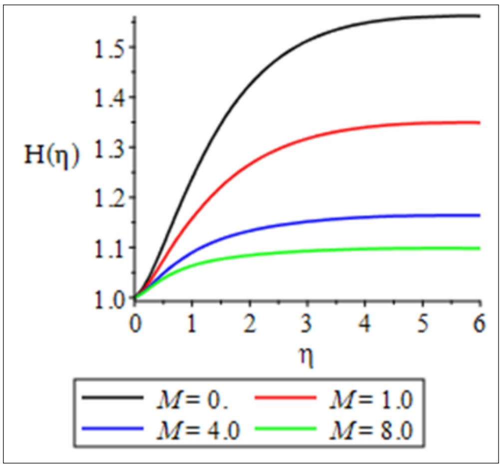

Figure 2 Effect of M on $\boldsymbol{H(\eta)}$

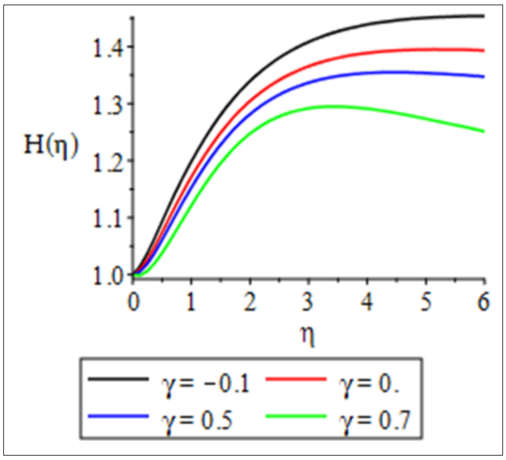

Figure 3 Effect of $\boldsymbol{\gamma}$ on $\boldsymbol{H(\eta)}$

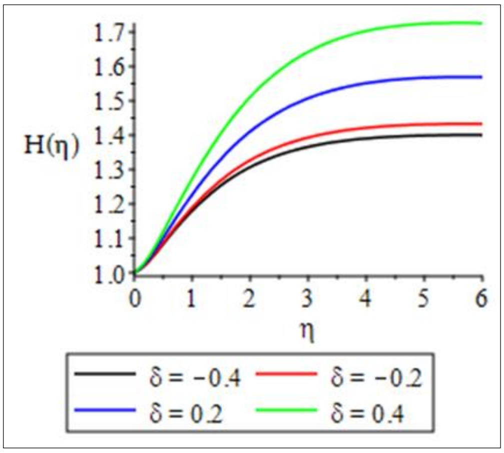

Figure 4 Effect of δ on $H(\eta)$

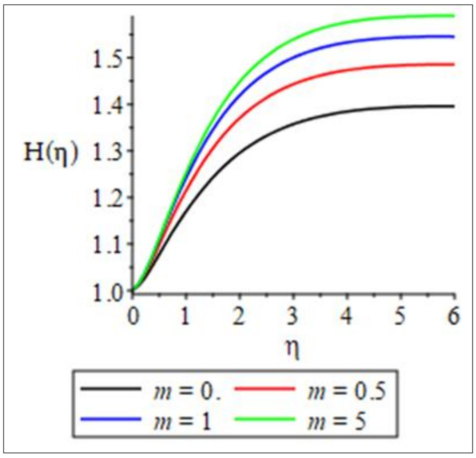

Figure 5 Effect of s on $H(\eta)$

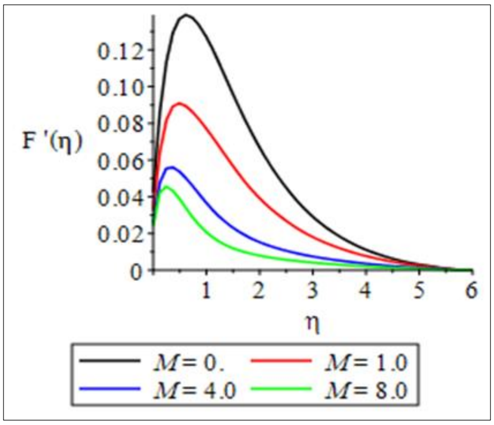

Figure 6 Effect of M on $\boldsymbol{F'(\eta)}$

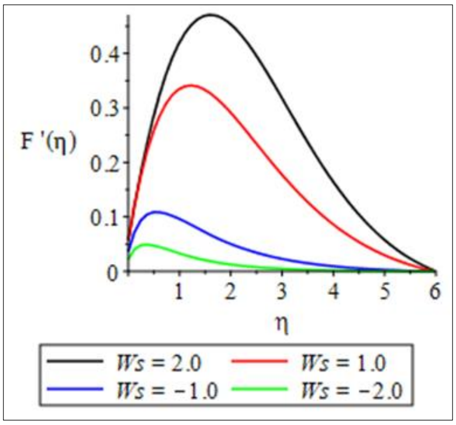

Figure 7 Effect of $\boldsymbol{W_s}$ on $\boldsymbol{F'(\eta)}$

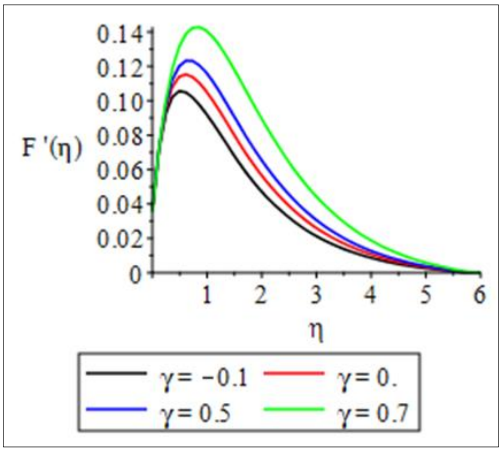

Figure 8 Effect of γ on $F'(\eta)$

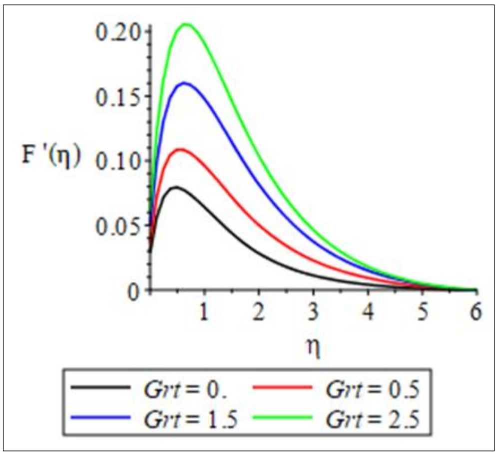

Figure 9 Effect of Grt on $F'(\eta)$

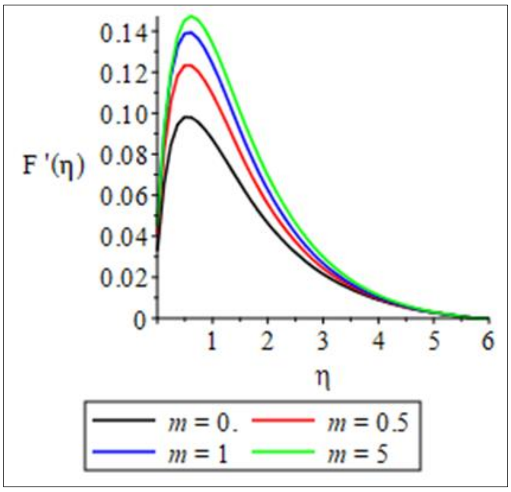

Figure 10 Effect of Grc on $F'(\eta)$

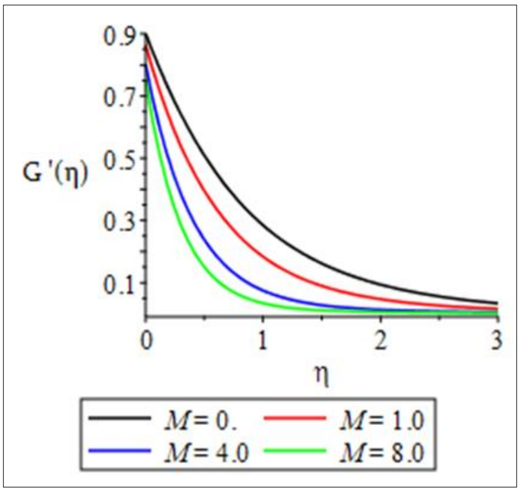

Figure 11 Effect of M on $G'(\eta)$

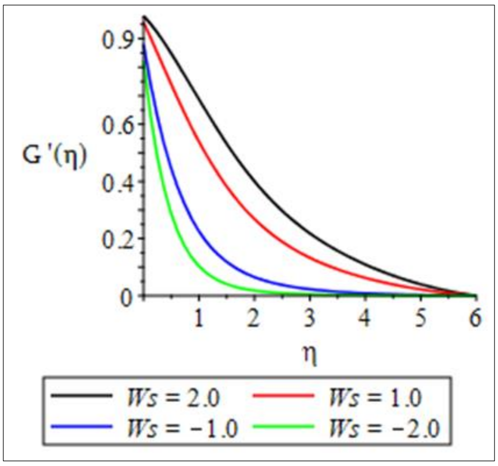

Figure 12 Effect of W_s on $G'(\eta)$

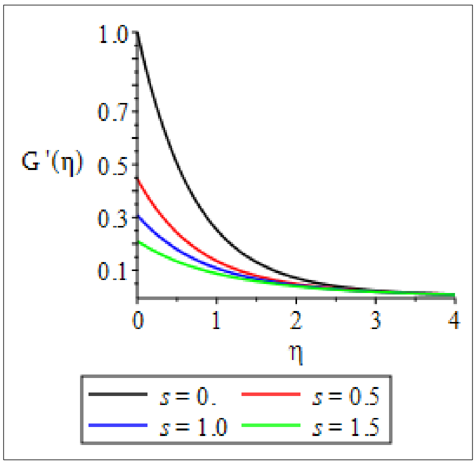

Figure 13 Effect of s on $G'(\eta)$

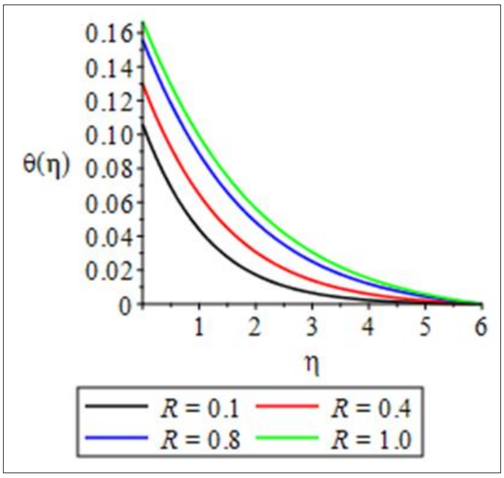

Figure 14 Effect of R on $\boldsymbol{\theta(\eta)}$

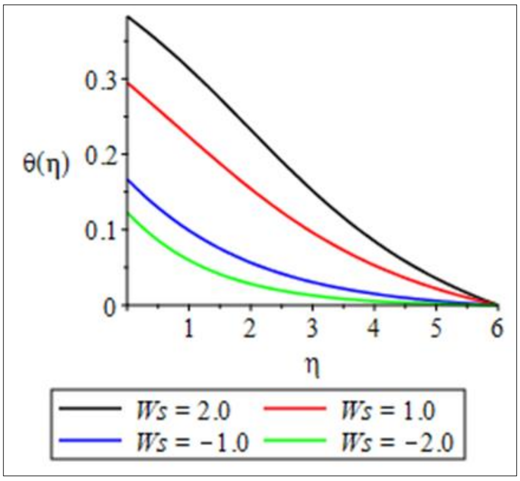

Figure 15 Effect of $\boldsymbol{W_s}$ on $\boldsymbol{\theta(\eta)}$

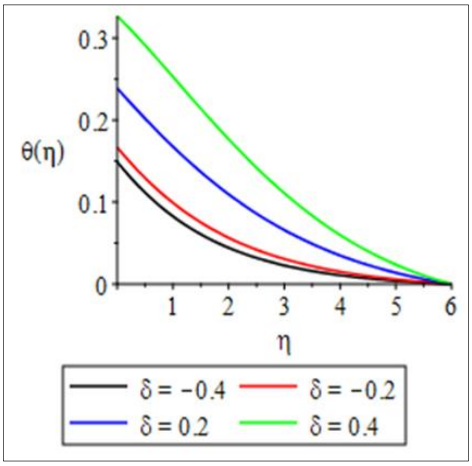

Figure 16 Effect of δ on $\theta(\eta)$

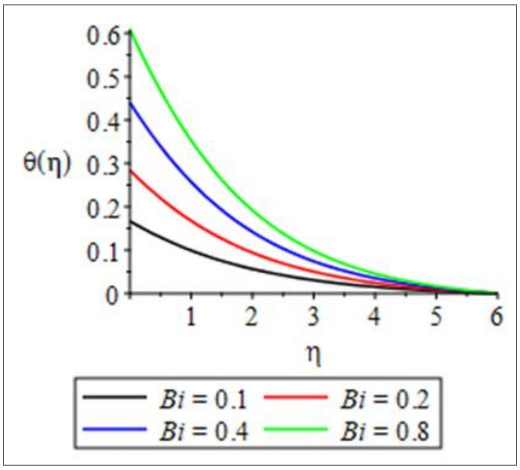

Figure 17 Effect of Bi on $\theta(\eta)$

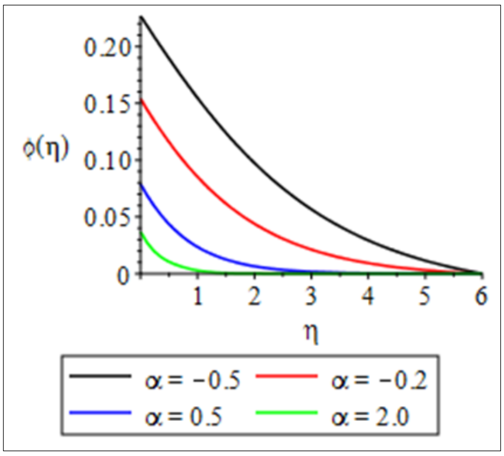

Figure 18 Effect of $\boldsymbol{\alpha}$ on $\boldsymbol{\phi(\eta)}$

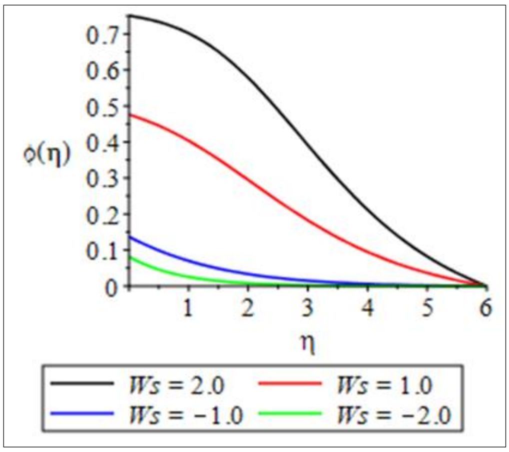

Figure 19 Effect of $\boldsymbol{W_s}$ on $\boldsymbol{\phi(\eta)}$

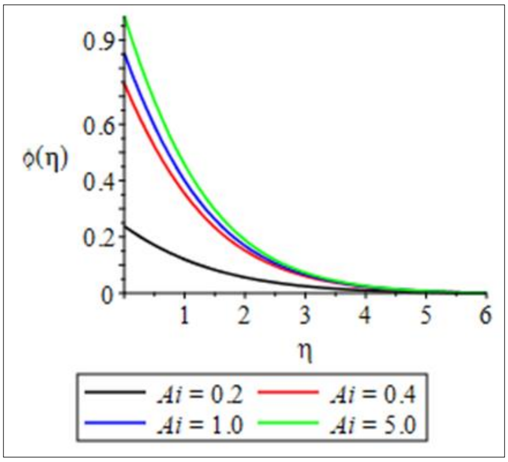

Figure 20 Effect of $\boldsymbol{Ai}$ on $\boldsymbol{\phi(\eta)v}$

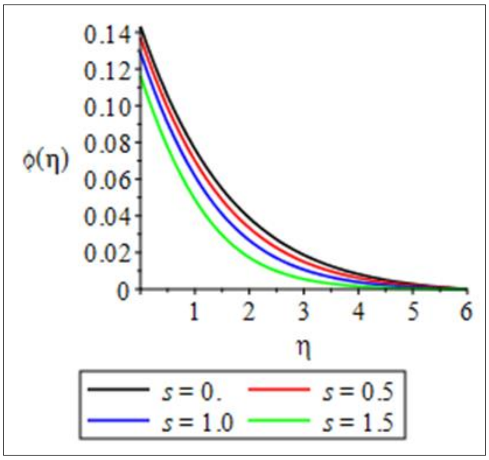

Figure 21 Effect of s on $\boldsymbol{\phi(\eta)}$

7. Results and discussions

As a result of the numerical calculations, the radial, tangential and axial velocities, with temperature and concentration distributions for the flow are obtained from Eqs. (17) – (22) and are displayed in Figures. 2–21 for different values of γ (relative temperature difference parameter), R (Thermal radiation parameter), Ws (suction /injection parameter), Bi (Magnetic field at the edge of the boundary layer) M (magnetic parameter), Grc (Species Grashof number) and Grt (Thermal Grashof number) etc respectively. In the present analysis the fluid considered is flue gas.

For flue gases ($Pr = 0.64$) the values of the exponents a, b and d are taken as $a = 0.7, b = 0.83$ and$d = -1.0$. $\gamma = \Delta T/T_\infty$ is termed as the relative temperature difference parameter, which is positive for a heated surface, negative for a cooled surface and zero for the case of constant property. In order to highlight the validity of the numerical computations adopted in the present investigation, some of our results for constant property case have been compared with those of Kelson and Desseaux [22] in Table 1. The comparisons show excellent agreements, hence an encouragement for the use of the present numerical computations.

The effects of γ on the radial and tangential velocity profiles are shown in Figures 3 and 8. In these Figures comparison is made between the constant property and variable property solutions from Figure. 3, it is seen that due to existence of the centrifugal force the radial velocity attains a maximum value close to the surface of the disk for all values of γ. The largest maximum value of the velocity is attained in case of the constant property (γ = 0).

Figure 3 also shows that very close to the disk surface an increase in the values of γ leads to the decrease in the values of the radial velocity while the opposing experience existed in Figure 8 as the values of γ increase. The effects of suction and injection (Ws) for $\gamma = 0.05$, $M = m = 0.05$ and $Pr = 0.64$ on the tangential, the axial velocity profiles, temperature and concentration profiles are shown in Figure 7, Figure 12, Figure 15 and Figure 19 respectively. For strong suction, tangential velocity and temperature decay rapidly away from the surface. It is no news that suction stabilizes the boundary layer as evident in these Figures. As for the injection (Ws > 0), from the Figures, it is observed that the boundary layer is increasingly blown away from the disk to form an interlayer between the injection and the outer flow regions. Also, it is found that temperature decay more slowly away from the surface. As in the case of temperature difference parameter, from Figure 12, we again observe that higher injection velocities have the tendency to destabilize the laminar flow. In Figure 7, it is observed that for high values of injection parameter (Ws = 4), the radial velocity near the disk is lower than that for smaller values of Ws. This is due to the fact that, with increasing values of Ws, the injected flow can sustain axial motion to greater distances from the wall. Then, near the wall, the radial flow which is fed by the axial flow is expected to decrease as the injected parameter increases.

Imposition of a magnetic field to an electrically conducting fluid creates a drag like force called the Lorentz force. This force has the tendency to slow down the flow around the disk at the expense of increasing its temperature. This is depicted by the decreases in the radial, tangential and axial velocity profiles and increases in the temperature profiles as M increases as shown in Figure. 5, Figure. 6, and Figure 11 respectively.

If the parametersγ,W□ and M are held constants, m illustrates the effect of Hall term on the flow. The parameter m has a marked effect on the velocity profiles as seen in Figure 5 and Figure 10. It is observed that, due to an increase in the magnitude of m within 0–2.0 (not precisely determined), both radial and axial velocity profiles increase. But if the magnitude of m is increased beyond the limit of 2.0 (possibly), the velocity profiles show a decreasing effect. This is due to the fact that for large values of m, the term $1/(1+m^2)$ is very small and hence the resistive effect of the magnetic field is diminished.

This phenomenon for small and large values of m has been effectively explained by Hassan and Attia [13]. From Figure 6(b) we observe that the Hall parameter m has slightly increasing effect on the tangential velocity profiles. The Hall current parameter m and magnetic interaction parameter M do not enter directly into the energy Eq. (16) but its influence come through the momentum Eqs. (14) and (15). Figure 5(d) and Figure. 6(d) show the small variation of temperature profiles for different values of M and m respectively. From Figure 5(d), it is observed that the value of non-dimensional temperature profile increases a little with the increasing values of M and this also leads to a small rate of increase in the thermal boundary layer thickness. The temperature profile decreases with the increasing values of Hall parameter m is shown in Figure. 6(d).

The influence of s is depicted by Figure 13 and Figure. 21, increasing the parameter influence velocity profiles by retarding both axial and tangential velocity profiles.

The effect of δ which is heat generation/absorption parameter is illustrated in Figure 4 and Figure. 16 where it is shown to influence both temperature profile and radial velocity profile positively, respectively. This is true because increasing values of the parameter increases thermal boundary layer and increases rate of mass and heat transfer across the boundary layers.

Figure 9 illustrates impact of thermal grashof numbers on tangential velocity profile. The graph shows that increasing values of the parameter increases tangential velocity profile.

Figure 12, Figure. 17, Figure 18 and Figure. 20 show effects of thermal radiation parameter, thermal slip parameter, mass heat generation/absorption parameter and mass slip parameter respectively. Increasing both values of radiation and thermal slip parameters increase the thermal boundary layer and causes rise in temperature profile along the disk as illustrated in Figure 12 and Figure. 17. Both mass heat generation/absorption parameter (Figure. 18) and mass slip parameter (Figure. 20) reduce transfer of species along the disk.

Table 1 Radial skin-friction, tangential skin-friction and the rate of heat transfer coefficients values comparison obtain $\boldsymbol{Sc=0.60, Pr=0.71, a=0.71, b=0.83, c=0.6, d=-1}$ when $\boldsymbol{M=0, m=0, \gamma=0, R=0.0, Grt=0.0, Grc=0.0, s=0, \delta=0.0, \alpha=0.0}$

Ws	**Maleque and Sattar (2005)**			**Kelson and Desseaux [22]**			**Current Work**		
	$F'(0)$	$G'(0)$	$\theta'(0)$	$F'(0)$	$G'(0)$	$\theta'(0)$	$F'(0)$	$G'(0)$	$\theta'(0)$
4.0	0.24304	0.02892	0.00001	0.24304	0.02892	0.00001	0.243063	-0.028926	-0.000119
3.0	0.30915	0.06029	0.00058	0.30915	0.06029	0.00058	0.309183	-0.060308	-0.002390
2.0	0.39893	0.13595	0.01105	0.39893	0.13595	0.01101	0.398981	-0.135962	-0.021414
1.0	0.48948	0.30217	0.08560	0.48948	0.30217	0.08488	0.489359	-0.302051	-0.103882
0.0	0.51014	0.61596	0.32953	0.51023	0.61592	0.32586	0.509440	-0.615664	-0.311832
-1.0	0.38941	1.17563	0.79768	0.38957	1.17522	0.79305	0.389061	-1.175767	-0.685383
-2.0	0.24328	2.04137	1.45065	0.24242	2.03853	1.43778	0.242380	-2.038738	-1.217534
-3.0	0.16684	3.01477	2.14906	0.16558	3.01214	2.13559	0.165574	-3.012194	-1.805309
-4.0	0.12766	4.00999	2.86448	0.12474	4.00518	2.84238	0.124737	-4.005196	-2.402249

Finally, the values of radial and tangential skin frictions and the rate of heat transfer have been presented in Tables 1 and 2. From Table 1, it can be seen that the values of the radial and tangential skin friction and the rate of heat transfer coefficients decrease for increasing values of injection velocity (Ws = 0 to 4). It also can be seen from this table that increasing the suction velocity (Ws = 0 to 4) leads to decrease in the radial skin friction coefficient while increase in the azimuthal (tangential) skin friction and the rate of heat transfer coefficients. It can be seen from Table 2 that the radial, the tangential and the rate of heat transfer coefficients decrease with the increasing values of temperature difference parameterγ.

Table 2 Radial skin-friction, tangential skin-friction, the rate of heat transfer and rate of mass transfer coefficients obtained for various values of $\boldsymbol{M}, \boldsymbol{R}, \boldsymbol{Ws}, \boldsymbol{\gamma}$ and $\boldsymbol{s}$

Para	$\boldsymbol{F'(0)}$	$\boldsymbol{G'(0)}$	$\boldsymbol{\theta'(0)}$	$\boldsymbol{\phi'(0)}$
$M = 0.0$	0.424583	-0.996991	-0.086776	-0.083648
$M = 1.0$	0.325602	-1.357740	-0.085974	-0.083099
$M = 4.0$	0.256346	-1.979484	-0.085149	-0.082598
$M = 8.0$	0.241231	-2.461821	-0.084804	-0.082405
$R = 0.1$	0.323160	-1.217599	-0.085927	-0.089405
$R = 0.4$	0.337693	-1.209021	-0.086062	-0.087012
$R = 0.8$	0.354877	-1.199511	-0.086228	-0.084416
$R = 1.0$	0.362491	-1.195433	-0.086302	-0.083316
$Ws = 2.0$	0.561859	-0.204136	-0.024916	-0.061714
$Ws = 1.0$	0.569094	-0.420139	-0.052347	-0.070487
$Ws = -1.0$	0.362491	-1.195433	-0.086302	-0.083316
$Ws = -2.0$	0.217889	-1.764740	-0.091887	-0.087698
$\gamma = -0.1$	0.362305	-1.237583	-0.086386	-0.083647
$\gamma = 0.0$	0.362080	-1.115373	-0.086167	-0.082642
$\gamma = 0.5$	0.360305	-1.023136	-0.086061	-0.081779
$\gamma = 0.7$	0.352252	-0.835211	-0.086094	-0.079650
$s = 0.0$	0.489447	-1.352393	-0.086186	-0.083243
$s = 0.5$	0.092528	-0.554129	-0.086328	-0.083327
$s = 1.0$	0.048738	-0.345588	-0.086281	-0.083296
$s = 1.5$	0.024992	-0.197256	-0.086251	-0.083276

Table 3 Radial skin-friction, tangential skin-friction, the rate of heat transfer and rate of mass transfer coefficients obtained for various values of $\boldsymbol{Grt}, \boldsymbol{Grc}, \boldsymbol{\delta}, \boldsymbol{Ai}, \boldsymbol{Bi}$ and $\boldsymbol{Pr}$

Para	$\boldsymbol{F'(0)}$	$\boldsymbol{G'(0)}$	$\boldsymbol{\theta'(0)}$	$\boldsymbol{\phi'(0)}$
$Grt = 0.0$	0.286915	-1.227351	-0.085693	-0.082921
$Grt = 0.5$	0.362491	-1.195433	-0.086302	-0.083316
$Grt = 1.5$	0.493700	-1.135626	-0.087115	-0.083902
$Grt = 2.5$	0.608077	-1.079851	-0.087659	-0.084333
$Grc = 0.1$	0.330669	-1.210164	-0.086085	-0.083172
$Grc = 0.4$	0.362491	-1.195433	-0.086302	-0.083316
$Grc = 0.8$	0.401903	-1.176640	-0.086547	-0.083484
$Grc = 1.4$	0.456200	-1.149885	-0.086849	-0.083699
$\delta = -0.4$	0.350675	-1.201985	-0.086191	-0.085101
$\delta = -0.2$	0.362491	-1.195433	-0.086302	-0.083316

$\delta = 0.2$	0.411139	-1.168699	-0.086739	-0.076122
$\delta = 0.4$	0.469860	-1.135675	-0.087203	-0.067305
$\alpha = -0.5$	0.410980	-1.177607	-0.077315	-0.083598
$\alpha = -0.2$	0.371109	-1.192154	-0.084607	-0.083365
$\alpha = 0.5$	0.336618	-1.206056	-0.092112	-0.083180
$\alpha = 2.0$	0.323832	-1.212424	-0.096316	-0.083129
$Ai = 0.2$	0.392792	-1.181035	-0.152400	-0.083446
$Ai = 0.4$	0.532489	-1.110854	-0.508742	-0.083973
$Ai = 1.0$	0.560052	-1.096326	-0.588260	-0.084065
$Ai = 5.0$	0.593478	-1.078514	-0.688764	-0.084173
$Bi = 0.1$	0.362491	-1.195433	-0.086302	-0.083316
$Bi = 0.2$	0.412289	-1.158716	-0.086616	-0.143159
$Bi = 0.4$	0.475580	-1.110520	-0.086967	-0.223883
$Bi = 0.8$	0.541077	-1.059091	-0.087286	-0.312436
$Pr = 0.01$	0.516680	-1.117638	-0.087634	-0.063022
$Pr = 0.71$	0.362491	-1.195433	-0.086302	-0.083316
$Pr = 4.00$	0.296330	-1.236819	-0.085734	-0.095184
$Pr = 7.00$	0.291153	-1.242083	-0.085721	-0.097037

Nomenclature

Parameter	**Definition**
x, y, z	coordinates
u, v, w	flow velocity components
P, P_∞,	Fluid pressure, constant pressure
r, ϕ, z	cylindrical polar coordinates
γ	relative temperature difference parameter
T, T_w, T_∞	fluid, uniform, and constant temperature
q	flow velocity
B, B_o	constant magnetic flux density, Induced magnetic field,
Bi	Magnetic field at the edge of the boundary layer
J, E	electric field
∇	Del or gradient symbol
Ω	constant angular velocity
U, U_o, U_w	Fluid, uniform and plate’s velocity
a, b, c, d	arbitrary exponent constants
k_s	Roseland mean absorption coefficient
μ_∞	uniform viscosity of the fluid
κ_∞	uniform thermal conductivity of heat
q, q_r	Fluid velocity, and fluid heat flux

η	Dimensionless variable
Bi, s, Ai	Thermal, Velocity and mass slip parameter
Q	Heat source
υ_f	fluid kinematic viscousity
μ, μ_∞	Viscosity, Velocity diffusivity
RE, Re, Re_m,	Local Reynolds number, rotational Reynolds number and small magnetic Reynolds number
τ_t, τ_r	tangential shear stress, surface (radial) stress
C, C∞, C_f,	Fluid concentration, constant concentration, and Skin friction coefficient
Nu	Nusselt number
n	normal direction to the wall
Ws	Suction/injection parameter
Sh	Sherwood number
H	Magnetic field parameter
Grt, Grc	Thermal, species Grashof number
λ	mean free path
α	Heat bsorption/generation parameter
β	Hall factor
δ	Heat generation/absorption
v_∞	uniform kinematic viscosity of the fluid
ξ	tangent momentum accommodation coefficient
Pr	Prandtl number
R	Thermal radiation parameter
e, n	charge of electron, electron concentration per unit volume
Sc	Schmidt number
H, F, G	Radial, tangential, axial velocity
θ	Dimensionless fluid temperature
ϕ	Dimensionless fluid concentration
ρ, ρ_∞	Density, constant pressure
μ	Dynamic viscosity
K, k	permeability parameter, thermal conductivity
Ce, Cp	Constant pressure specific heat
ρ cp	Heat capacity
σ, σ*	Electrical conductivity, Stefan Boltzmann constant
M, m	Magnetic, Hall current parameter
R, Pr	Radiation, prandtl number
Dm,	Mass Diffusion
Ww, Ut, Kn	tangent velocity, Knudsen Number

8. Conclusion

In this paper, the effects of variable properties along with the effects of suction/injection and Hall current on a steady MHD convective flow induced by an infinite rotating porous disk were studied. The Nachtsheim and Swigert iteration technique based on sixth-order Range–Kutta and Shooting method has been employed to complete the integration of the resulting solutions.

The following conclusions can be drawn as a result of the computations:

- Variable properties (γ) has marked effects on the radial and axial velocity profiles. Close to the surface of the disk these velocities slow down as c increases but shortly after they increase with the increase of γ.
- Due to the existence of the centrifugal force, the radial velocity reaches a maximum value close to the surface of the disk.
- Close to the boundary positive values of γ is found to give rise to the familiar inflection point profile leading to the destabilization of the laminar flow. Strong injection also leads to the similar destabilization effect.
- The effect of Lorentz force or the usual resistive effect of the magnetic field on the velocity profiles is apparent.
- Hall parameter m has an interesting effect on the radial and axial velocity profiles. For large values of $m(> 2.0)$, the resistive effects of the magnetic field is diminished and hence the radial and axial velocity profiles decreases with the increase of m.
- Increasing the values of γ (1.0 to 1.0) lead to the decrease in radial and tangential skin friction coefficients and the rate of heat transfer coefficient for fixed values of Ws, M, m and Pr.

Compliance with ethical standards

Acknowledgments

The management of Igbinedion University, Okada is appreciated and thanked by the writers for providing conducive environment and research facilities. We also appreciate the unnamed referees' helpful comments, which helped to improve the final product.

Disclosure of conflict of interest

The authors declare that they have no known competing financial interests or personal relationships that could have appeared to influence the work reported in this paper.

References

[1] J. Herrero, J.A.C. Humphrey, F. Giralt, Comparative analysis of coupled flow and heat transfer between corotating discs in rotating and fixed cylindrical enclosures, Am. Soc. Mech. Eng., Heat Transfer Div. 300 (1994) 111– 121.

[2] J.M. Owen, R.H. Rogers, Flow and heat transfer in rotating disc system, Rotor–Stator Systems, vol. 1, Research Studies Press, Taunton, UK and John Wiley, NY, 1989.

[3] T. von Kar`man`, Uber laminare und turbulente reibung, ZAMM 1 (1921) 233–255.

[4] W.G. Cochran, The flow due to a rotating disc, Proc. Cambridge Phil. Soc. 30 (1934) 365–375.

[5] E.R. Benton, On the flow due to a rotating disc, J. Fluid Mech. 24 (Part-4) (1965) 781–800.

[6] M.G. Roger, G.N. Lance, The rotationally symmetric flow of a viscous fluid in presence of infinite rotating disc, J. Fluid Mech. 7 (1960) 617–631.

[7] G.K. Batchelor, Note on a class of solutions of the Navier–Stokes equations representing steady non-rotationally symmetric flow, Quart. J. Mech. Appl. Math. 4 (1951) 29–41.

[8] J.T. Stuart, On the effect of uniform suction on the steady flow due to a rotating disc, Quart. J. Mech. Appl. Math. 7 (1954) 446–457.

[9] H. Ockendon, An asymptotic solution for steady flow above an infinite rotating disc with suction, Quart. J. Mech. Appl. Math. 25 (1972) 291–301.

[10] H.K. Kuiken, The effect of normal blowing on the flow near a rotating disk of infinite extent, J. Fluid Mech. 47 (4) (1971) 789–798.

[11] T.M.A. El-Mistikawy, H.A. Attia, A.A. Megahed, The rotating disk flow in the presence of weak magnetic field, in: Proc. Fourth Conf. Theoret. Appl. Mech., Cairo, Egypt, 5–7 November, 1991, pp. 69–82.

[12] T.M.A. El-Mistikawy, H.A. Attia, The rotating disk flow in the presence of strong magnetic field, in: Proc. Third int. Cong. Fluid Mech., Cairo, Egypt, 2–4 January, 3, 1990, pp. 1211–1222.

[13] A.L.A. Hassan, Hazem Ali Attia, Flow due to a rotating disk with Hall effect, Phys. Lett. A 228 (1997) 246–290.

[14] Hazem Ali Attia, Unsteady MHD flow near a rotating porous disk with uniform suction or injection, Fluid Dyn. Res. 23 (1998) 283–290.

[15] M. Zakerullah, J.A.D. Ackroyd, Laminar Natural Convection Boundary Layers on Horizontal Circular discs, J. Appl. Math. Phys. 30 (1979) 427–435.

[16] H. Herwig, The effect of variable properties on momentum and heat transfer in a tube with constant heat flux across the wall, Int. J. Heat Mass Transfer 28 (1985) 424–441.

[17] H. Herwig, G. Wickern, The effect of variable properties on laminar boundary layer flow, Warme und Stoffubertragung 20 (1986) 47–57.

[18] H. Herwig, K. Klemp, Variable property effects of fully developed laminar flow in concentric annuli, ASME J. Heat Transfer 110 (1988) 314–320.

[19] H. Herwig, An asymptotic analysis of laminar film boiling a vertical plate including variable property effects, Int. J. Heat Mass Transfer 31 (1988) 2013–2021.

[20] P.R. Nachtsheim, P. Swigert, Satisfaction of asymptotic boundary conditions in numerical solution of system of nonlinear of boundary layer type. NASA TN-D3004, 1965.

[21] S. Jayaraj, Thermophoresis in laminar flow over cold inclined plates with variable properties, Heat Mass Transfer 30 (1995) 167–173.

Author's short biography

	**Raphael Ehikhuemhen Asibor** Has Ph.D in Computational Fluid Dynamics. Has his Master's degree from Olabisi Onabanjo University, Ago-Iwoye Ogun State and a Doctor of Philosophy in Mathematics from Ambrose Alli University, Ekpoma, Edo State, Nigeria. A Researcher in Combustion, Magneto and Heat Transfer. Member of IAENG, NAMP, MAN etc. Currently the Director of ICT, Igbinedion University, Okada and have attended and participated actively in many local and international conferences and workshops.
	**Celestine Friday Osuidia** completed his Bachelor of Science (BSc) and masters of Science (MSc) degree in Industrial mathematics both from the great Ambrose Alli University, Ekpoma, Edo State, Nigeria in the year 2012 and 2017 respectively. He is now working as an Education Officer, Master II, Tutor in Delta State Post Primary Education Board, Asaba, Delta state, Nigeria. At this appointment he is deeply involved in the teaching of basic and fundamental principles of mathematics. His areas of research are concerned with developing and finding the most efficient mathematical methods to solve problems arising in industrial settings.